



NASA TM-80111

# NASA Technical Memorandum 80111

NASA-TM-80111 19790019546

## COMPUTER PREDICTIONS OF PHOTOCHEMICAL OXIDANT LEVELS FOR INITIAL PRECURSOR CONCENTRATIONS CHARACTERISTIC OF SOUTHEASTERN VIRGINIA

N. T. WAKELYN AND ALLEN G. McLAIN

JUNE 1979

**LIBRARY COPY**

JUL 9 1979

LANGLEY RESEARCH CENTER  
LIBRARY, NASA  
HAMPTON, VIRGINIA



National Aeronautics and  
Space Administration

**Langley Research Center**  
Hampton, Virginia 23665



NF00665

1 Report No NASA TM-80111		2 Government Accession No		3 Recipient's Catalog No	
4 Title and Subtitle COMPUTER PREDICTIONS OF PHOTOCHEMICAL OXIDANT LEVELS FOR INITIAL PRECURSOR CONCENTRATIONS CHARACTERISTIC OF SOUTHEASTERN VIRGINIA				5 Report Date June 1979	
				6 Performing Organization Code	
7 Author(s) N. T. Wakelyn and Allen G. McLain				8 Performing Organization Report No	
9 Performing Organization Name and Address NASA Langley Research Center Hampton, Va. 23665				10 Work Unit No 146-20-10-07	
				11 Contract or Grant No	
12 Sponsoring Agency Name and Address National Aeronautics and Space Administration Washington, D.C. 20546				13 Type of Report and Period Covered Technical Memorandum	
				14 Sponsoring Agency Code	
15 Supplementary Notes					
16 Abstract  A computer study has been performed with a photochemical box model, using a contemporary chemical mechanism and procedure, and a range of initial input pollutant concentrations thought to encompass those characteristic of the Southeastern Virginia region before a photochemical oxidant episode. The model predictions are consistent with the expectation of high summer afternoon ozone levels when initial nonmethane hydrocarbon (NMHC) levels are in the range 0.30-0.40 ppmC and NO <sub>x</sub> levels are in the range 0.02-0.05 ppm. Calculations made with a Lagrangian model, for one of the previously calculated cases, which had produced intermediate afternoon ozone levels, suggest that urban source additions of NMHC and NO <sub>x</sub> exacerbate the photochemical oxidant condition.					
17 Key Words (Suggested by Author(s)) Computer simulation Photochemical modeling Ozone <u>Environment Pollution</u>			18 Distribution Statement  Unclassified - Unlimited  Subject Category 45		
19 Security Classif (of this report) Unclassified	20 Security Classif (of this page) Unclassified	21 No of Pages 31	22 Price* \$4.50		

COMPUTER PREDICTIONS OF PHOTOCHEMICAL OXIDANT LEVELS  
FOR INITIAL PRECURSOR CONCENTRATIONS CHARACTERISTIC  
OF SOUTHEASTERN VIRGINIA

N. T. Wakelyn and Allen G. McLain  
Langley Research Center

SUMMARY

A computer study has been performed with a photochemical box model, using a contemporary chemical mechanism and procedure, and a range of initial input pollutant concentrations thought to encompass those characteristic of the Southeastern Virginia region before a photochemical oxidant episode. The model predictions are consistent with the expectation of high summer afternoon ozone levels when initial nonmethane hydrocarbon (NMHC) levels are in the range 0.30 - 0.40 ppmC and NO<sub>x</sub> levels are in the range 0.02 - 0.05 ppm. Calculations made with a Lagrangian model, for one of the previously calculated cases, which had produced intermediate afternoon ozone levels, suggest that urban source additions of NMHC and NO<sub>x</sub> exacerbate the photochemical oxidant condition.

INTRODUCTION

The Southeastern Virginia region regularly experiences high photochemical oxidant concentrations (refs. 1 and 2) during the summer months. This condition is characterized by a general southwesterly flow of air into the region and bright "blue sky" days occurring in conjunction with a high-pressure cell. The constancy of summer weather presents an opportunity for the test of airborne and satellite instrumentation in a large and predictable area containing rural, urban, and water regions. The Southeastern Virginia Urban Plume Study of the summer of 1977 (ref. 3) was instituted to utilize the area as a test bed for remote sensors currently under development by the NASA and its contractors. A variety of ozone levels are measurable in the region from early morning levels as low as about 0.030 ppm to late afternoon levels which can reach, from time-to-time, almost 0.200 ppm (refs. 2 and 3).

In order to fully utilize the potential of the data from such a study, photochemical models of the region must be employed to test the reasonableness and consistency of the various inputs to the data base. As a beginning effort in the development and test of a photochemical model, a finite rate chemical kinetics package was modified to vary the rate coefficients of the unimolecular photolytic decompositions in a diurnal manner. The package is capable of handling unimolecular, bimolecular, and termolecular chemistry and is provided with a stiff ordinary differential equation solver (ref. 4). Provision for time-varying source inputs of pollutant species, mixed-layer rise dilution, and restart and off-line plotting capability was also written into the computer code.

N79-27717 #

A computer exercise was performed using a contemporary, chamber-verified chemical mechanism (refs. 5 and 6), a box-type model similar to that described in reference 7, and a test procedure (ref. 8) of merit. Input for the exercise spanned that range of common pollutant species concentrations generally thought to be characteristic of the Southeastern Virginia area during the morning preceding an afternoon photochemical oxidant incident. Preliminary calculations were also made with a Lagrangian (moving air parcel, ref. 8) model to determine the effect of a range of consistent source inputs on oxidant levels for the region. The purpose was to test the compatibility of the mechanism, model, and procedure and to obtain predictions and trends which could be compared to data obtained from future field experiments. A family of curves was generated of predicted ozone levels as a function of initial  $\text{NO}_x$  and nonmethane hydrocarbon (NMHC) input as well as source (time varying) inputs of these substances, with diurnal variation of the photolytic rates. The present paper is concerned with the results of these calculations.

### THE CHEMICAL MECHANISM

The chemical kinetic mechanism used in this computer simulation consists of photochemical decompositions, inorganic rearrangements, organic oxidation reactions (with "lumping" of organics into paraffins and olefins), and reactions describing the rearrangements of oxidized organics. A rather complete sensitivity analysis is presented in reference 6. The following unimolecular photochemical decompositions, with the rate coefficients calculated by the method of reference 9 and varied every 5 minutes over the course of the simulation, were used:

	$k, * \text{ min}^{-1}$
1. $\text{NO}_2 \rightarrow \text{NO} + \text{O}$	2.036E-1
2. $\text{HNO}_2 \rightarrow \text{OH} + \text{NO}$	1.182E-2
3. $\text{HNO}_3 \rightarrow \text{NO}_2 + \text{OH}$	2.233E-6
4. $\text{H}_2\text{O}_2 \rightarrow \text{OH} + \text{OH}$	4.520E-4
5. $\text{RCHO} \rightarrow \text{stable products}$	1.594E-3
6. $\text{RCHO} \rightarrow 1/2 \text{RO}_2 + 3/2 \text{HO}_2$	1.594E-3

\*0800 l.d.t. (local daylight time), Hampton, Virginia, latitude 36.85  
Longitude 76.35, August 4, 1977, "blue sky."

The photolytic rate coefficients and their diurnal variation over a 10-hour period are shown in figure 1.

The inorganic rearrangements (from ref. 6) used are as follows:

	$k, \text{ ppm}^{-x} \text{ min}^{-1} (x = 0,1)$
7. $\text{O} + (\text{O}_2) \rightarrow \text{O}_3$	3.30E+6
8. $\text{O}_3 + \text{NO} \rightarrow \text{NO}_2 + \text{O}_2$	2.10E+1
9. $\text{O}_3 + \text{NO}_2 \rightarrow \text{NO}_3 + \text{O}_2$	4.60E-2
10. $\text{NO}_3 + \text{NO} \rightarrow 2 \text{NO}_2$	1.50E+4
11. $\text{NO}_2 + \text{NO}_3 + (\text{H}_2\text{O}) \rightarrow 2 \text{HNO}_3$	4.50E+0
12. $\text{O} + \text{NO} \rightarrow \text{NO}_2$	2.50E+3
13. $\text{O} + \text{NO}_2 \rightarrow \text{NO} + \text{O}_2$	1.40E+4
14. $\text{O} + \text{NO}_2 \rightarrow \text{NO}_3$	3.00E+3
15. $\text{NO} + \text{NO}_2 + (\text{H}_2\text{O}) \rightarrow 2 \text{HNO}_2$	1.50E-2
16. $2 \text{HNO}_2 \rightarrow \text{NO} + \text{NO}_2 + \text{H}_2\text{O}$	1.10E+0
17. $\text{OH} + \text{NO}_2 \rightarrow \text{HNO}_3$	6.00E+3
18. $\text{OH} + \text{NO} \rightarrow \text{HNO}_2$	4.80E+3
19. $\text{HO}_2 + \text{NO} \rightarrow \text{OH} + \text{NO}_2$	7.00E+2

The oxidation of hydrocarbons to produce aldehydes and alkyl and acyl peroxide radicals is described by the following reaction set for olefins (ref. 6)

	$k, \text{ ppm}^{-1} \text{ min}^{-1}$
20. $\text{OLEF} + \text{OH} \rightarrow \text{RCHO} + \text{RO}_2$	2.50E+4
21. $\text{OLEF} + \text{O} \rightarrow \text{RO}_2 + 1/2 \text{HO}_2 + 1/2 \text{RCO}_3$	6.80E+3
22. $\text{OLEF} + \text{O}_3 \rightarrow \text{RCHO} + \text{RCO}_3 + \text{OH}$	1.60E-2

and, for paraffins (ref. 5).

23. $\text{PARA} + \text{OH} \rightarrow \text{RO}_2 + \text{H}_2\text{O}$	3.80E+3
24. $\text{PARA} + \text{O} \rightarrow \text{RO}_2 + \text{OH}$	6.50E+1

The hydrocarbon mechanism was described by the referenced workers as smog chamber verified and specialized for automobile exhaust. As one would expect, the rate coefficients for reactions involving olefins are greater than those involving paraffins (olefins > paraffins) and  $\text{OH} > \text{O} > \text{O}_3$ .

The rearrangement of oxidized organics to produce, in part, PAN and alkyl nitrite and nitrate is described by the following set (ref. 6)

	$k, \text{ppm}^{-x} \text{min}^{-1} (x = 0,1)$
25. $\text{RCHO} + \text{OH} \rightarrow 1/2 \text{RCO}_3 + 1/2 \text{HO}_2$	2.30E+4
26. $\text{RO}_2 + \text{NO} \rightarrow \text{RO} + \text{NO}_2$	3.00E+3
27. $\text{RCO}_3 + \text{NO} \rightarrow \text{RO}_2 + \text{NO}_2$	1.50E+3
28. $\text{RCO}_3 + \text{NO}_2 \rightarrow \text{PAN}$	5.00E+2
29. $\text{RO} + (\text{O}_2) \rightarrow \text{RCHO} + \text{HO}_2$	5.00E+3
30. $\text{RO} + \text{NO}_2 \rightarrow \text{RONO}_2$	4.90E+2
31. $\text{RO} + \text{NO} \rightarrow \text{RONO}$	2.50E+2
32. $2 \text{HO}_2 \rightarrow \text{H}_2\text{O}_2 + \text{O}_2$	5.30E+3
33. $\text{RO}_2 + \text{HO}_2 \rightarrow \text{RO} + \text{OH} + \text{O}_2$	1.00E+2
34. $2 \text{RO}_2 \rightarrow 2 \text{RO} + \text{O}_2$	1.00E+2

#### MODELS AND TEST PROCEDURE

There are tropospheric models in current use or under development of varying complexity in their description of atmospheric diffusion and chemistry. For example, see reference 10. In the event of inadequate meteorological data (a common occurrence) or for the purpose of emphasizing the chemistry part of the problem with a minimum of mathematical difficulty, a box (ref. 7), multi-box (ref. 11), or traveling air parcel (ref. 8) model can be used as the modeling tool. Since the purpose of the current computer study is to test the compatibility of a contemporary chemical scheme and test procedure with a range of initial input data for a region of interest, and to find trends which could help plan and interpret future data gathering studies, the box concept was used for the bulk of the work with some calculations performed with a traveling air parcel model.

The procedure used in the computer simulation, essentially that of reference 8, is as follows

a. Nonmethane hydrocarbons were taken to be a mix of olefin (propylene) and paraffin (n-butane) in such proportion as to simulate the reactivity of automobile emissions 25 percent propylene (ppmC) + 75 percent n-butane (ppmC).

b. Aldehydes were assumed to be 5 percent of the initial NMHC levels (in ppmC).

c. All computer simulations were 10 hours long, beginning at 0800 l.d.t.

d. Photolytic rate coefficients were varied every 5 minutes in accordance with diurnal variation in sunlight from 0800 - 1800 l.d.t. Mixed-layer dilutions method of reference 9 (see fig. 1).

e. An atmospheric dilution rate, due to mixed layer rise, of 3 percent per hour was assumed for the period 0800 - 1500 l.d.t. Mixed-layer dilutions for S.E. Virginia are generally substantially greater than this.

f. Following the suggestion of reference 12.

$$\text{Initial NO}_x \begin{cases} \text{NO}_2 = 0.25 \text{ NO}_x \\ \text{NO} = 0.75 \text{ NO}_x \end{cases}$$

Calculations were also performed without atmospheric dilution and with a different ratio of NO<sub>2</sub> and NO for NO<sub>x</sub> in order to illustrate the magnitude of these effects. (See appendices A and B.)

#### Photochemical Box Model

The photochemically reacting volume under consideration in the box model is conceived as being rectangular in form, length not necessarily equal to width, and with a varying height to account for mixed layer rise. Since no provision for ground scavenging of ozone is provided in the present form of the model, the bottom of the box is at a position some 10 meters above ground level. The box is oriented such that the front face is normal to the wind direction, the initial concentration of pollutants and precursors at the front face is characteristic of the box as a whole, and any calculated concentration changes are homogeneously applied over the entire box. Photochemistry is calculated by marching forward in time from 0800 l.d.t. while changing the photolytic rate coefficients and outputting results every 5 minutes.

The box model used in this study does not consider sources within the modeled region and thus, by implication, only applies to over water and rural areas north of Norfolk. The traveling air-parcel model to be described later does not suffer from this inadequacy. Aside from the fact that current knowledge of local sources of NO<sub>x</sub> and NMHC is less than satisfactory, there is need to know what ozone levels can result from the initial input alone. This baseline value of what levels of oxidant are to be expected after several hours of photochemical reaction, irrespective of local precursor contribution, is the concern of the major portion of this study.

## Traveling Air Parcel Model

To determine the effect of source loadings on eventual ozone levels, several calculations were performed with what, in essence, is a Lagrangian (traveling air parcel) model. The same procedure and photochemical mechanism was used for both the present model and the previously discussed photochemical box model. A parcel of air, with initial  $\text{NO}_x$  and NMHC concentrations of one of the intermediate (in ozone generation) cases previously calculated with the photochemical box model, enters the Norfolk area from the southwest, is in the Norfolk area and subject to source additions of  $\text{NO}_x$  and NMHC for a 2-hour period (0800 - 1000 l.d.t.), and then passes out over the water where sources are "turned off" and where it photochemically ages for the rest of the simulation. The 2-hour period is consistent with the urban area size and prevailing windspeed. Proportionate source contributions, with instant homogeneity assumed, were made every 5 minutes of the Lagrangian simulation. In keeping with the suggestion of reference 7, the following ratio is used for primary emissions of oxides of nitrogen:  $\text{NO}_2/\text{NO}_x = 0.10$  and  $\text{NO}/\text{NO}_x = 0.90$ .

## RESULTS AND DISCUSSION

### Photochemical Box Model

The range of pollutant species concentrations thought to be characteristic of the Southeastern Virginia region on a summer's morning before an afternoon photochemical oxidant incident is depicted in table I. A NMHC  $\text{NO}_x$  ratio of from 5 to 20 is considered characteristic of an urban area (ref. 12).

NMHC NO <sub>x</sub>				
	0.10	0.20	0.30	0.40
0.050	2.0	4.0	6.0	8.0
0.040	2.5	5.0	7.5	10.0
0.030	3.3	6.7	10.0	13.3
0.020	5.0	10.0	15.0	20.0

Table I.- Range of initial NMHC (ppmC) and  $\text{NO}_x$  (ppm) levels used in simulation and their associated NMHC :  $\text{NO}_x$  ratios

Computer simulations were made for the 16 combinations of  $\text{NO}_x$  and nonmethane hydrocarbons, as initial conditions, with  $\text{NO}_x$  varying from 0.020 - 0.050 ppm and NMHC varying from 0.10 to 0.40 ppmC. The characteristic incoming ozone is typically from 0.030 - 0.060 ppm (ref. 2). The simulations were based upon an initial ozone value of 0.050 ppm. Variations of ozone concentration with time for four initial  $\text{NO}_x$  inputs are shown in figure 2 (a, b, c, d), with each figure representing a different



initial NMHC concentration. What appears to be a dip in the ozone concentration at 1500 hours for all the curves is the point in time at which mixed layer dilutions are no longer taken. For all of these simulations, there is an initial decline in ozone levels due to reaction number 8. This decline is an indication that an initial ozone concentration of 0.050 ppm is incompatible with initial  $\text{NO}_x$  in the 0.020 - 0.050 ppm range and with 75 percent of this  $\text{NO}_x$  being NO. Calculations with initial  $\text{NO}_2$  taken to be 80 percent of the initial  $\text{NO}_x$  showed no initial decline for any simulation. The results of calculations with this ratio are presented in Appendices A and B, with and without mixed layer rise.

The lowest NMHC case, figure 2a, indicates that 0.100 ppmC does not represent sufficient NMHC to discriminate between various  $\text{NO}_x$  levels; in fact, an unexpected inverse trend between  $\text{O}_3$  and initial  $\text{NO}_x$  is displayed. No doubt, part of the explanation of the inverse trend lies in the establishment of a consistent  $\text{O}_3/\text{NO}/\text{NO}_2$  pattern, that is, a mixture that would not undergo a rapid change. The 0.200 ppmC NMHC case, figure 2b, displays a direct relationship between  $\text{O}_3$  and  $\text{NO}_x$  after 2 hours of simulation, except for the highest  $\text{NO}_x$  levels. Figure 2 (c and d), 0.300 and 0.400 ppmC of NMHC, displays a direct and increasingly severe relationship between  $\text{O}_3$  and initial  $\text{NO}_x$ . With NMHC greater than 0.200 ppmC,  $\text{NO}_x$  in the range 0.020 - 0.050 ppm produces the expectation of an afternoon oxidant episode in the context of the model.

Figure 3 (a, b, c, d) is a cross-plotting of what was presented in figure 2. The different plots show the change in ozone concentration with time and varying initial NMHC concentration, with a different initial  $\text{NO}_x$  concentration for each plot. Except for the lowest  $\text{NO}_x$  concentration, figure 3a, and highest NMHC concentration (and then only after about 500 minutes) for this figure, there is a direct relationship between  $\text{O}_3$  and initial NMHC concentration. An especially severe relationship exists at the highest  $\text{NO}_x$  level, figure 3d (0.050 ppm  $\text{NO}_x$ ).

While an inverse relationship can exist between  $\text{O}_3$  production and initial NMHC and  $\text{NO}_x$  concentration, the predominant relationship for the concentration range of the simulation (table I) is a direct one. One could also inquire if  $\text{O}_3$  production is related to the NMHC/ $\text{NO}_x$  ratio and could observe in table I three cases in which this ratio is 10.0. The corresponding curves, however, in figures 2 or 3 show no particular significance for the ratio of NMHC to  $\text{NO}_x$  within the range of concentrations used in the simulation.

#### Traveling Air Parcel Model

Using an intermediate case as a base, sources were added during the first 2 hours of simulation as a representation of an air parcel passing over an urban area. The intermediate case consisted of the following initial conditions:  $\text{NO}_x$  0.030 ppm, NMHC 0.200 ppmC, and  $\text{O}_3$  0.050 ppm. These concentrations are probably high compared to normal background levels. Figure 4 displays the variation of ozone concentration with time for a NMHC loading of  $108.8 \mu\text{g m}^{-3} \text{ hr}^{-1}$ \* and with the  $\text{NO}_x$  loading varying from

---

\*  $1.0 \text{ ppm} = (1.2187 \times 10^4) \frac{(\text{mole weight}) \mu\text{g}}{(\text{T}, \text{K}) \text{ m}^3}$

5.44 to 21.8  $\mu\text{g m}^{-3} \text{ hr}^{-1}$ . Figure 5 displays the variation of ozone concentration with time for a  $\text{NO}_x$  loading of 5.44  $\mu\text{g m}^{-3} \text{ hr}^{-1}$  and with the NMHC loading varying from 54.4 to 217.6  $\mu\text{g m}^{-3} \text{ hr}^{-1}$ . A NMHC loading at the 54.4  $\mu\text{g m}^{-3} \text{ hr}^{-1}$  level is consistent with the yearly regional loading of 100,000 tons. The  $\text{NO}_x$  loading was varied over a range of values to produce a change in ozone production. Any increase in  $\text{NO}_x$  or NMHC over the initial range of concentrations produces an increase in photochemical oxidant over the previously calculated case with the exception of the highest NMHC loadings of figure 5.

#### CONCLUDING REMARKS

Computer predictions of ozone concentration for 10-hour photochemical simulations, beginning at 0800 l.d.t., have been calculated as a function of initial  $\text{NO}_x$  and nonmethane hydrocarbon (NMHC) input concentrations. A contemporary chemical mechanism (including diurnally varied rate coefficients for six photochemical decompositions) and procedure (which specifies, in part, an assumed constitution of  $\text{NO}_x$  and NMHC) were used in these photochemical box-model calculations. The range of precursor species concentrations used in the simulations ( $\text{NO}_x$  varying from 0.020 to 0.050 ppm and NMHC varying from 0.100 to 0.400 ppmC) is generally thought to span that characteristic of the Southeastern Virginia region on a summer morning before an afternoon photochemical oxidant episode. With the exception of the lowest values for the NMHC, afternoon photochemical oxidant concentrations greater than 0.010 ppm are predicted by the model. All photochemical box-model calculations predict a rising ozone level from morning to afternoon with the concentration varying between 0.040 and 0.200 ppm, which is consistent with observations in the Southeastern Virginia region. It should be noted, however, that the present calculations present a worst case (highest ozone) situation since the contemporary procedure assumes a lower dilution rate than is probable. That the chamber produced chemical scheme yields predictions consistent with observations for such a crude model lends encouragement to the development of models with more sophisticated meteorology and to the obtaining of more exact species concentration data.

Since the initial input to the model, which begins in the morning with rural air, is necessarily aged air with pollutant precursors generated the previous day, it is thought that the initial  $\text{NO}_x$  should be characterized by a higher proportion of  $\text{NO}_2$  than that used in the simulation ( $\text{NO}_2 : \text{NO} = 1:3$ ). The computer simulation is consistent with this idea as is shown by the initial decline in ozone for all cases. However, peak ozone is not affected significantly by the initial proportions of  $\text{NO}_x$ . As a corollary thought, since n-butane is less reactive with oxidants in air than propylene, the proportion of propylene to n-butane, representing the initial input of NMHC to the model, should be lowered such that there is a greater proportion of n-butane in the representation of NMHC. This would result in lowered ozone production since the revised NMHC mixture would be less reactive.

Simulations with the Lagrangian (traveling air parcel) model yield relatively higher ozone levels than those with photochemical box model since they are, in effect, a coupling of an intermediate box-model calculation with 2-hour source additions of  $\text{NO}_x$  and NMHC. The mid-range of

the assumed initial precursor concentrations has such a potential for oxidant production that any additional contribution of either  $\text{NO}_x$  or NMHC would lead to significant increases in ozone.

The initial  $\text{NO}_x$  and NMHC concentrations were represented in the calculations by certain ratios of  $\text{NO}_2$  to NO and propylene to n-butane, respectively, as were the source additions (though not necessarily by the same ratios). It is felt that the use of these assumed ratios can represent a significant source of error, with the use justified only by its allowing calculation with insufficient data; for example, hydrocarbon data are available only as methane and total hydrocarbon concentrations, not concentrations of individual hydrocarbons. In view of the development of detailed chemical mechanisms for the hydrocarbons, it is believed, along with others (see, for example, A. C. Lloyd, NASA RP 1022, pp. 278-279, 1978) (ref. 13), that the requirement exists for much more detailed air quality data measurements. It is also clearly evident that other critical inputs are accurate solar insolation, emissions inventory, and meteorological data.

## APPENDIX A

The changes in ozone concentration with time for various initial  $\text{NO}_x$  concentrations are shown in this section. These calculations were made assuming a  $\text{NO}_2/\text{NO}_x$  ratio of 0.80. This ratio of  $\text{NO}_2$  to  $\text{NO}_x$  did not produce the initial decline of ozone during the first few minutes of the simulation. The implication is that the original  $\text{NO}_2$  to  $\text{NO}_x$  ratio used was not consistent with the initial assumption of 0.050 ppm  $\text{O}_3$ .

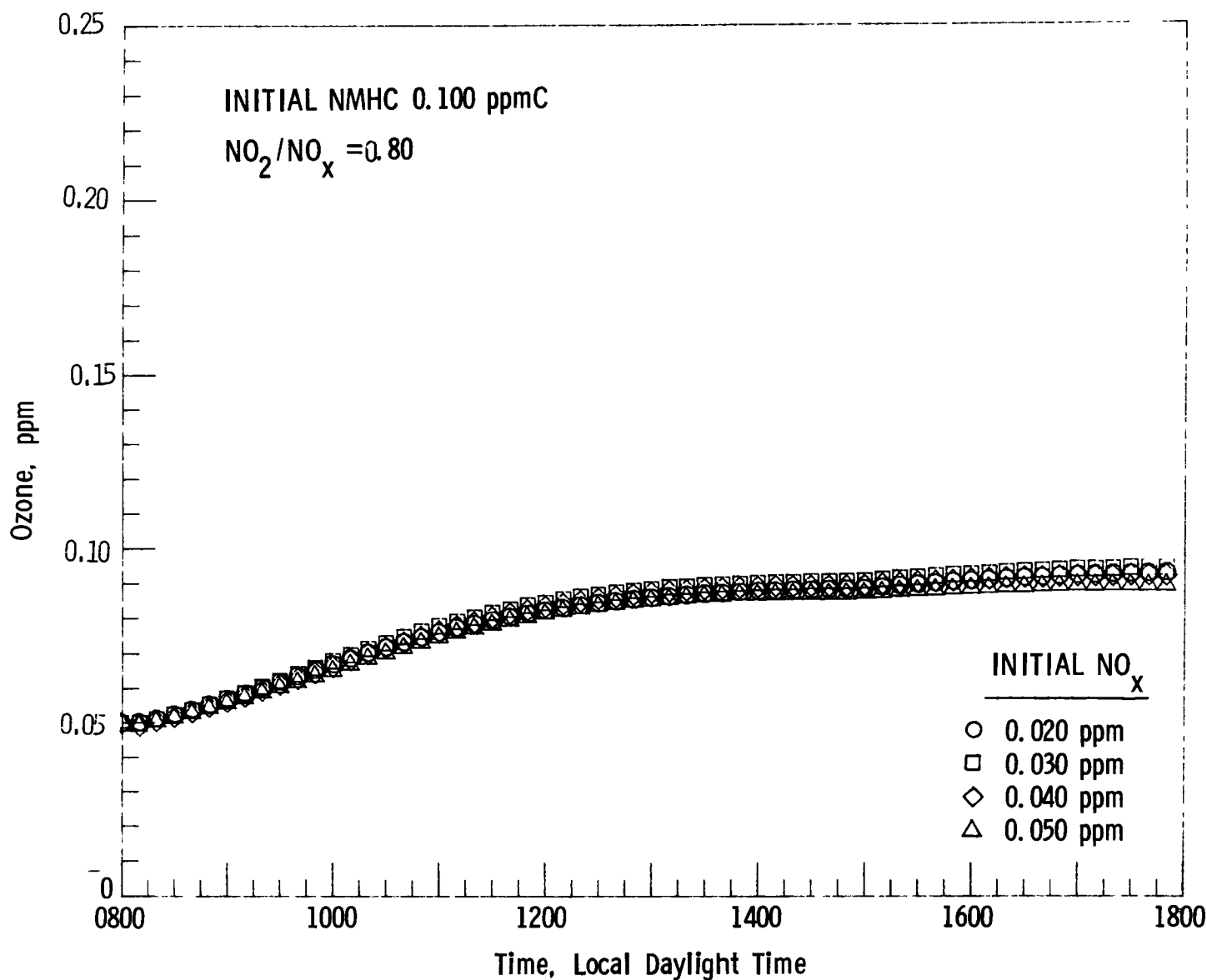


Figure A1. - Change of  $\text{O}_3$  concentration with time for various initial  $\text{NO}_x$  concentrations.

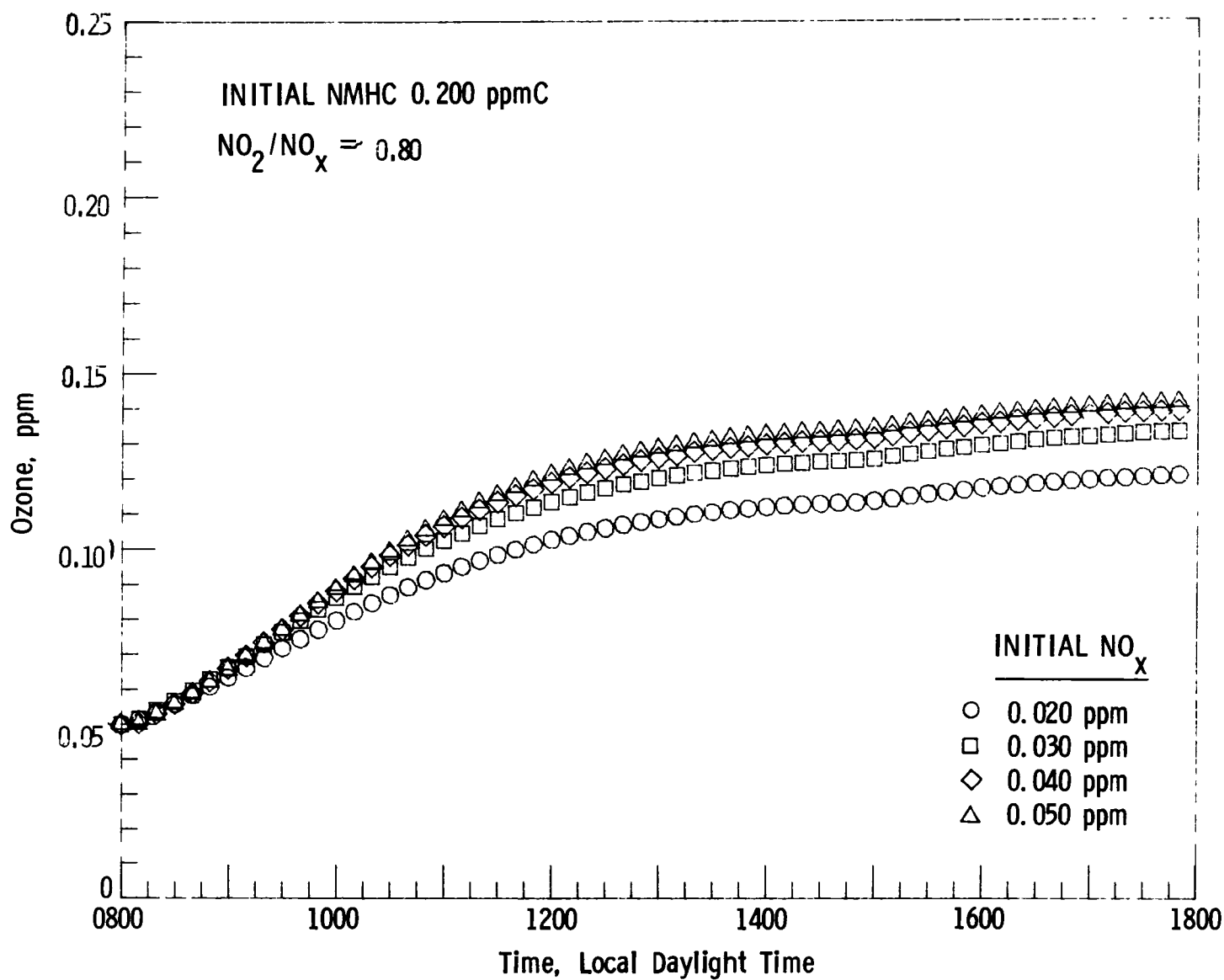


Figure A2. - Change of  $\text{O}_3$  concentration with time for various initial  $\text{NO}_x$  concentrations.

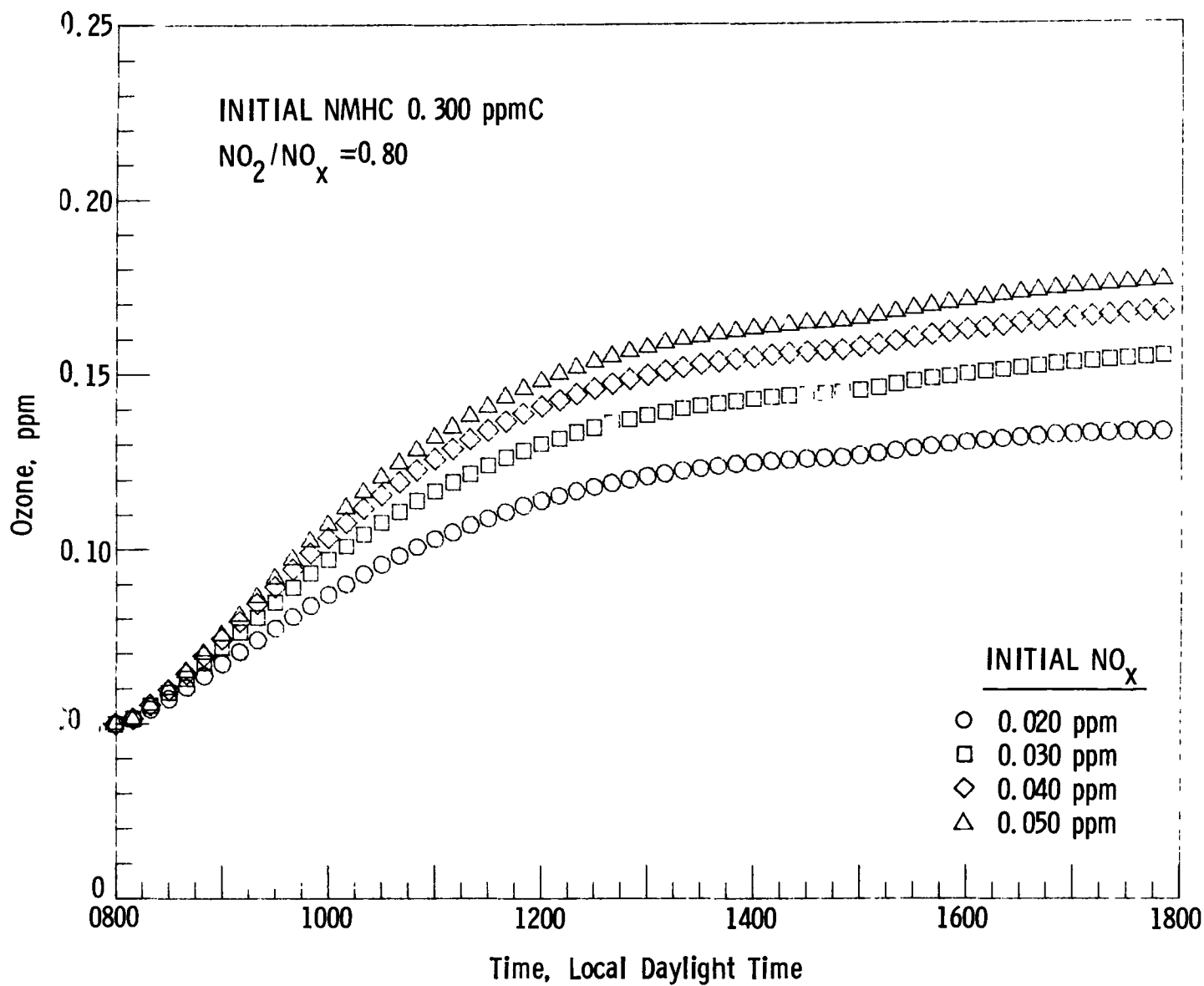


Figure A3. - Change of  $\text{O}_3$  concentration with time for various initial  $\text{NO}_x$  concentrations.

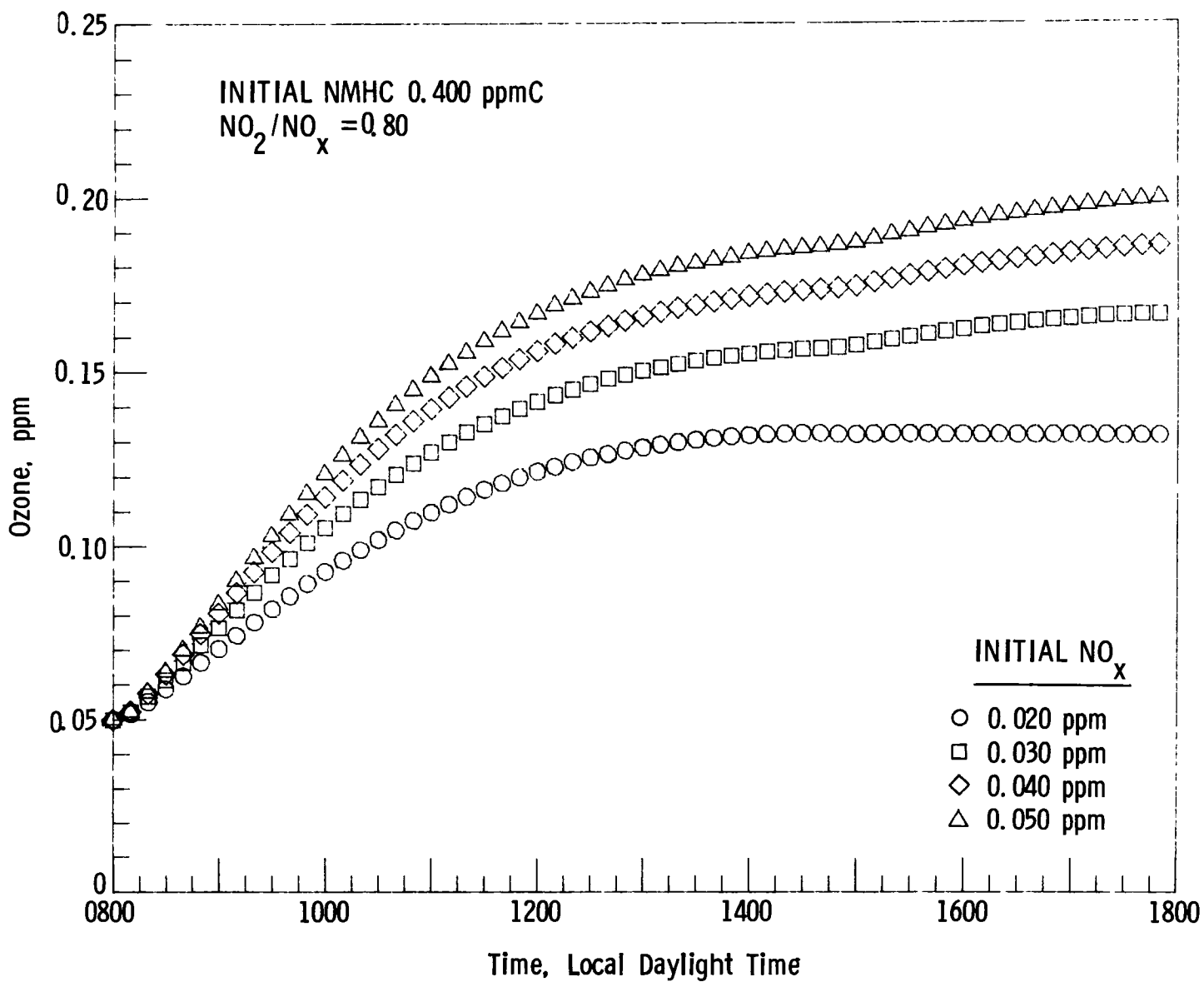


Figure A4. - Change of  $\text{O}_3$  concentration with time for various initial  $\text{NO}_x$  concentrations.



## APPENDIX B

The changes in ozone concentration with time for various initial  $\text{NO}_x$  concentrations are shown in this section. These calculations were made assuming a  $\text{NO}_2/\text{NO}_x$  ratio of 0.80; however, dilution from mixed layer height rise was not included. With no dilution, the levels of ozone concentration are higher than cases where the mixing layer height was allowed to change.

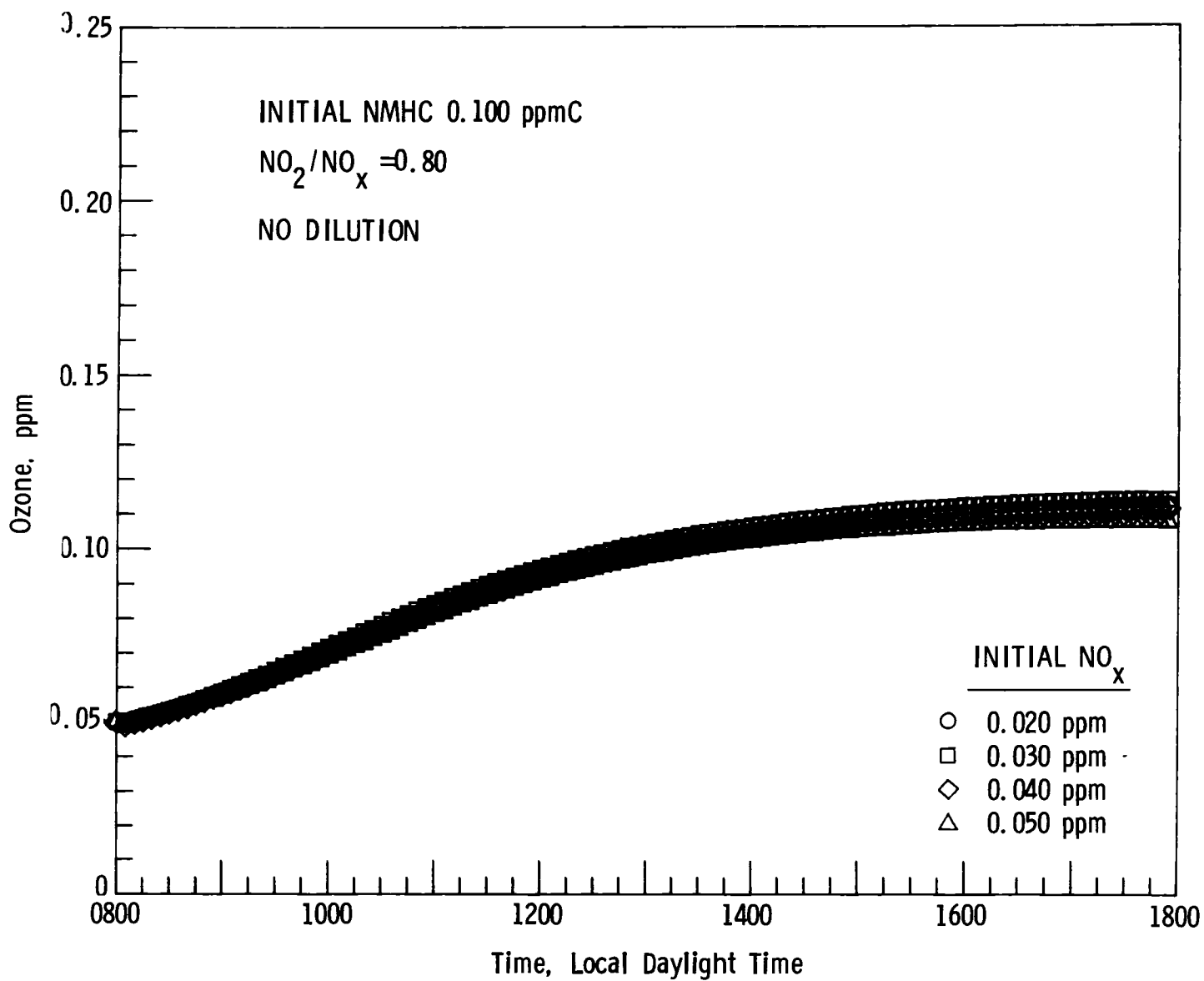


Figure B1. - Change of  $\text{O}_3$  concentration with time for various initial  $\text{NO}_x$  concentrations.

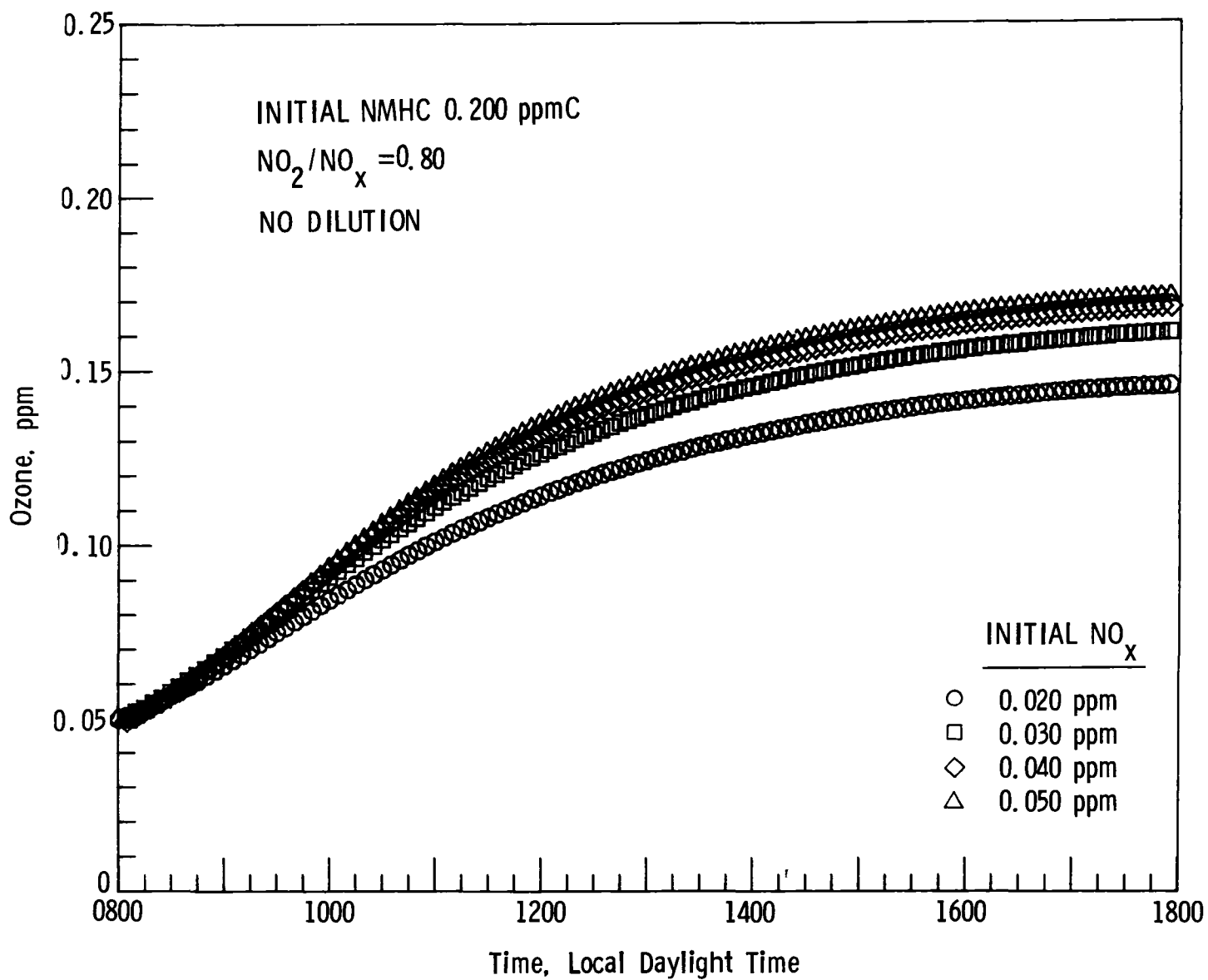


Figure B2. - Change of  $\text{O}_3$  concentration with time for various initial  $\text{NO}_x$  concentrations.

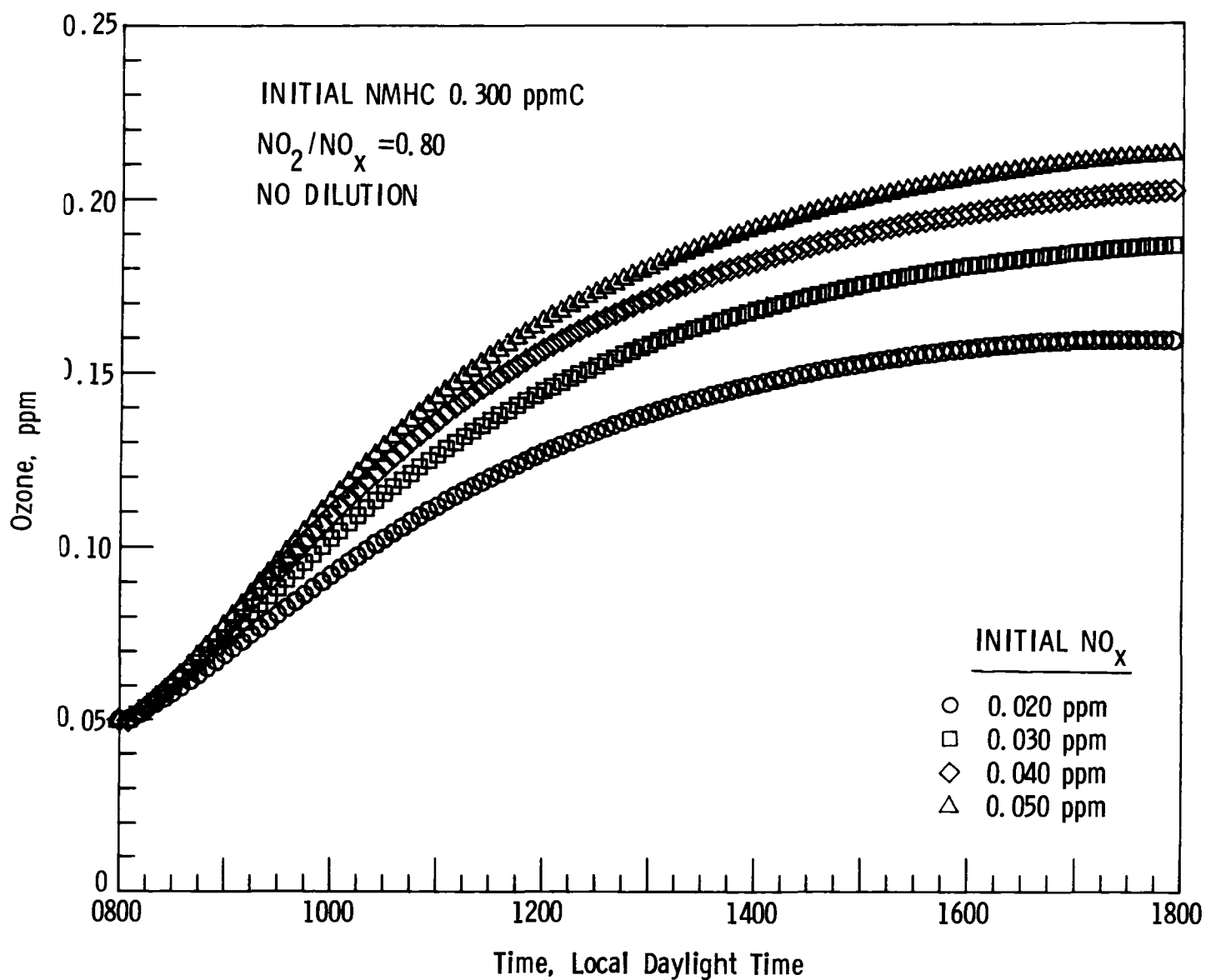


Figure B3. - Change of  $\text{O}_3$  concentration with time for various initial  $\text{NO}_x$  concentrations.

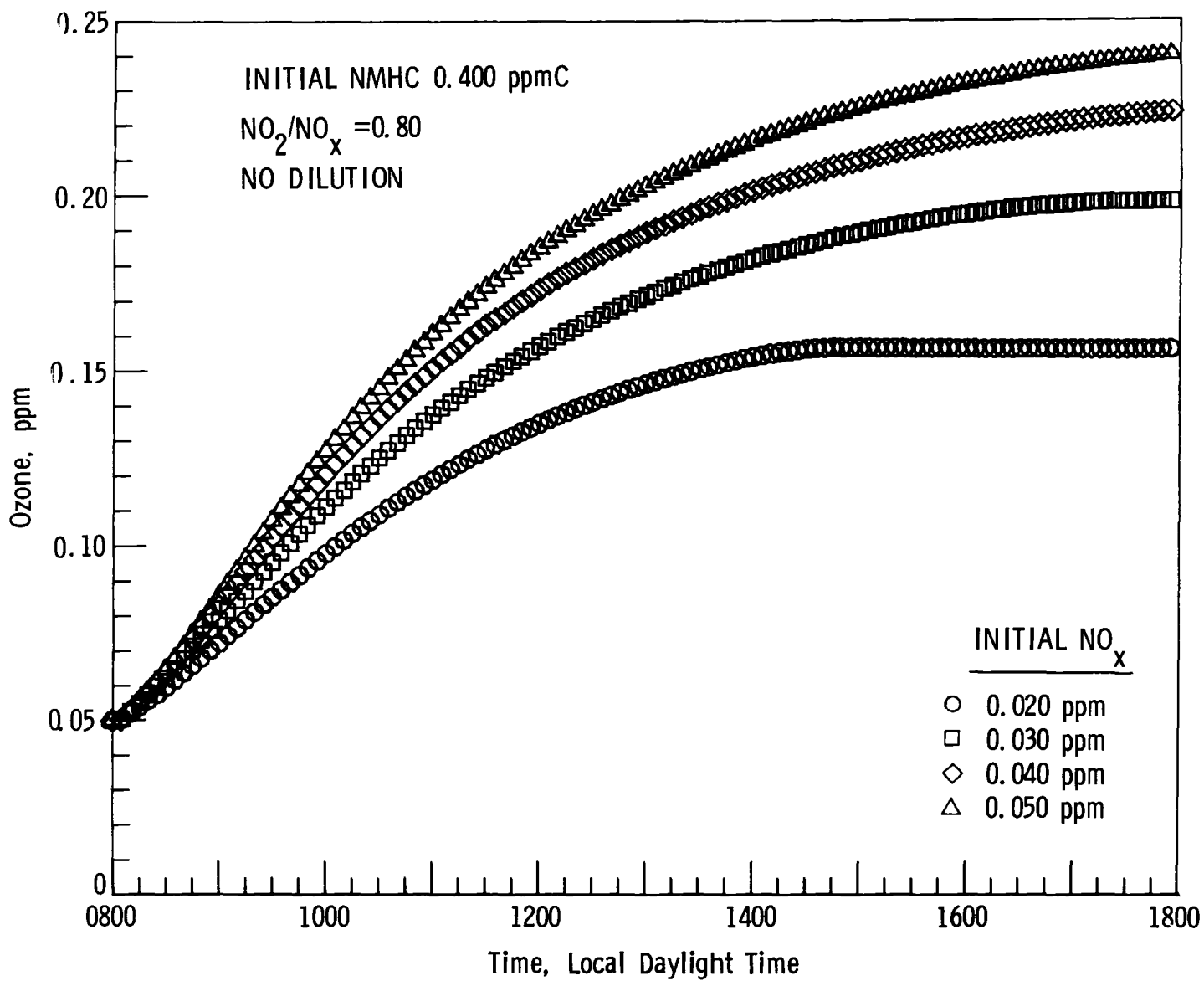


Figure B4. - Change of  $\text{O}_3$  concentration with time for various initial  $\text{NO}_x$  concentrations.

## REFERENCES

1. EPA-Released State Air Quality Data Show Areas Not Meeting Federal Standards. Journal of the Air Pollution Control Association, vol. 28, no. 4, Apr. 1978, pp. 378-380.
2. DeMarrais, Gerard A.: The Ozone Problem in the Norfolk, Virginia Area. EPA-600/4-78-006, Jan. 1978.
3. Wagner, H. S., Gregory, G. L., and Buglia, J. J.: The Southeastern Virginia Urban Plume, A Test Site for Remote Sensors. Seventy-first Annual Meeting of the Air Pollution Control Association, Houston, TX, June 25-29, 1978.
4. Gear, C. William: Numerical Initial Value Problems in Ordinary Differential Equations. Prentice-Hall, Inc., c1971.
5. Hecht, Thomas A.; Seinfeld, John H., and Dodge, Marcia C.. Further Development of Generalized Kinetic Mechanism for Photochemical Smog. Environmental Science and Technology, vol. 8, no. 4, Apr. 1974, pp. 327-339.
6. Dodge, M. C. and Hecht, T. A. Rate Constant Measurements Needed to Improve a General Kinetic Mechanism for Photochemical Smog. International Journal of Chemical Kinetics, Symposium No. 1, 1975.
7. Schere, K. L. and Demerjian, K. L. A Photochemical Box Model for Urban Air Quality Simulation. Proceedings of the Fourth Joint Conference on Sensing of Environmental Pollutants, New Orleans, LA, Nov. 6-11, 1977, pp. 427-433.
8. Meyers, E. L., Jr.; Summerhays, J.E.; and Freas, W. P.. Uses, Limitations and Technical Basis of Procedures for Quantifying Relationships Between Photochemical Oxidants and Precursors. U.S. EPA Publication No. EPA-450/2-77-021a, Nov. 1977.
9. Schere, Kenneth, L. and Demerjian, Kenneth L. Calculation of Selected Photolytic Rate Constants over a Diurnal Range. EPA-600/4-77-015, Mar. 1977.
10. Demerjian, K. L.. Photochemical Air Quality Simulation Modeling: Current Status and Future Prospects. International Conference on Photochemical Oxidant Pollution and Its Control Proceedings, Raleigh, NC, vol. I, Sept. 12-17, 1976.
11. Graedel, T. E., Farrow, L. A., and Weber, T. A. Kinetic Studies of the Photochemistry of the Urban Troposphere. Atmospheric Environment, vol. 10, 1976, pp. 1095-1116.
12. Dodge, Marcia C. Effect of Selected Parameters on Predictions of a Photochemical Model. EPA-600/3-77-048, June 1977.
13. Lloyd, Alan C. The Role of Computer Modeling of Photochemical Smog in Defining Existing Measurement Needs. NASA RP-1022, 1978, pp. 278-279.

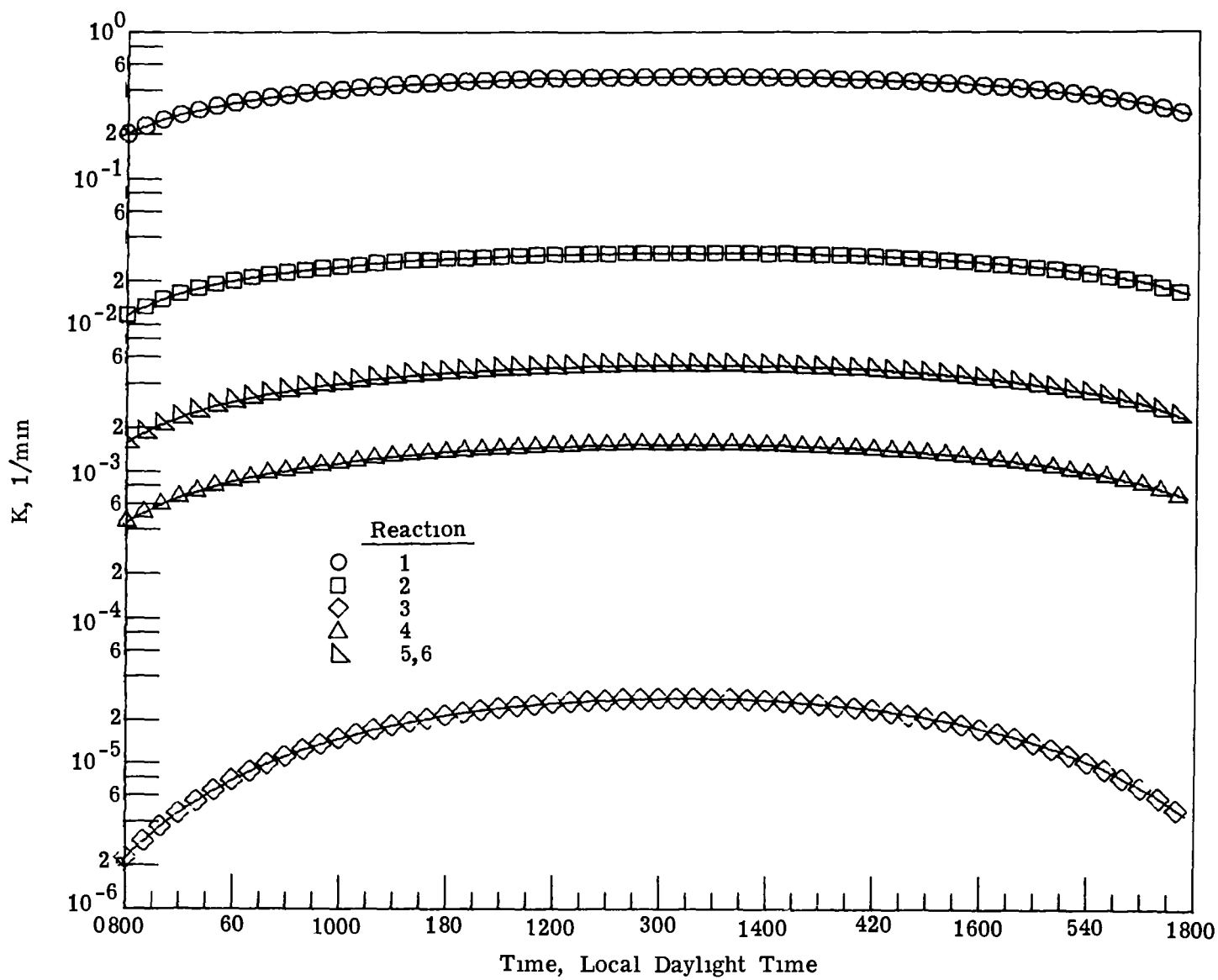


Figure 1.- Diurnal variation of the photolytic rate coefficients.

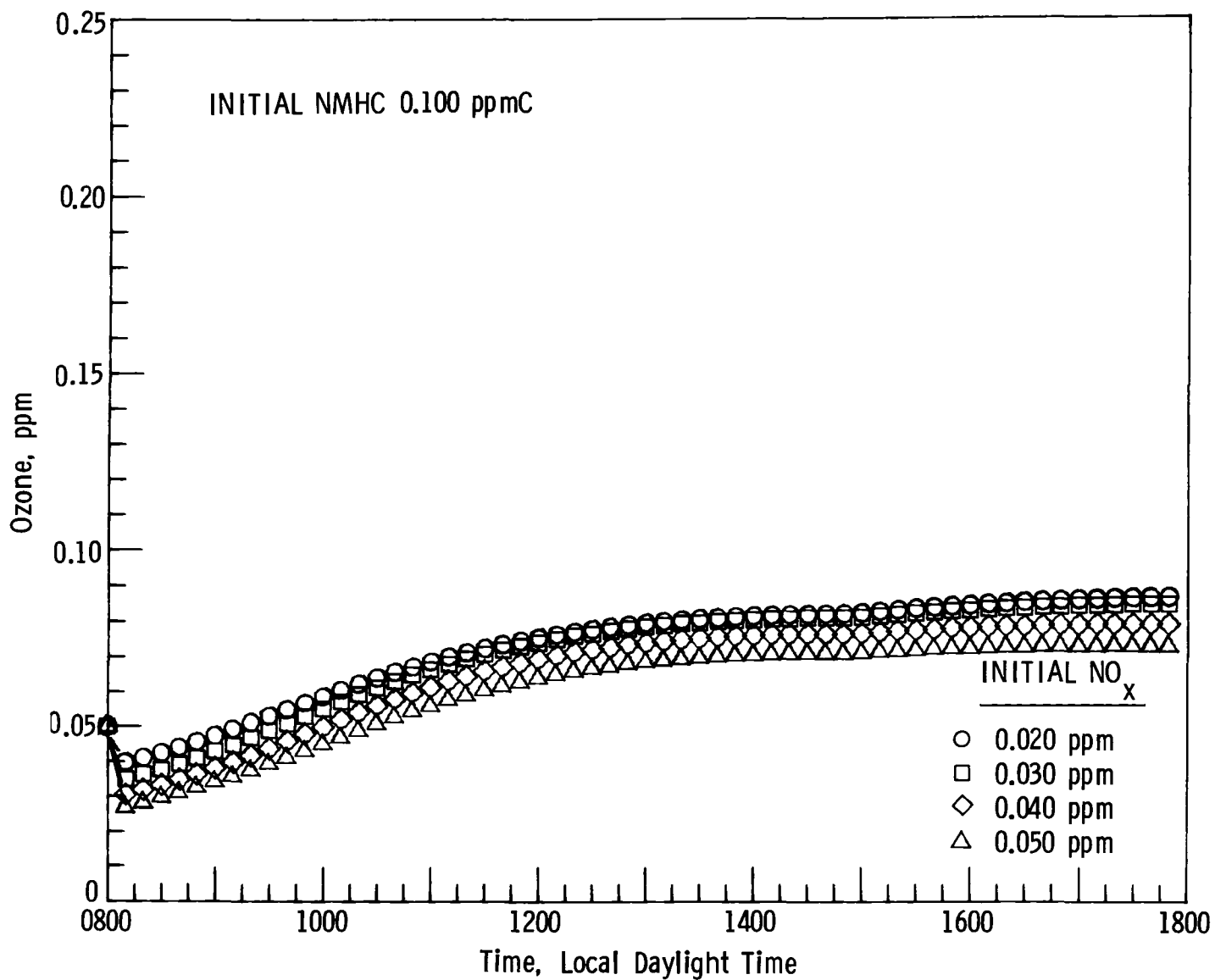


Figure 2a.- Change of O<sub>3</sub> concentration with time for various initial NO<sub>x</sub> concentrations.



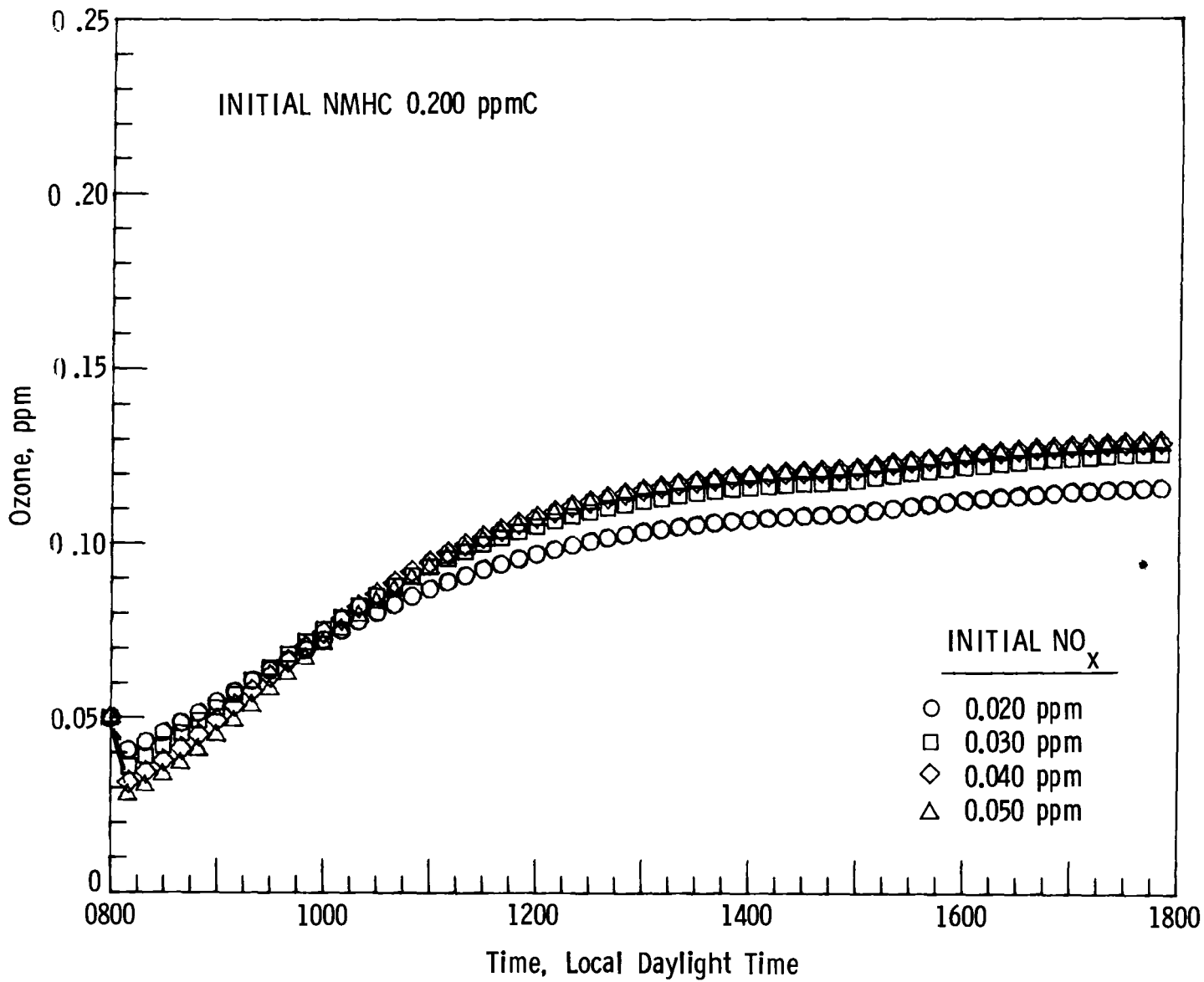


Figure 2b.- Change of O<sub>3</sub> concentration with time for various initial NO<sub>x</sub> concentrations.

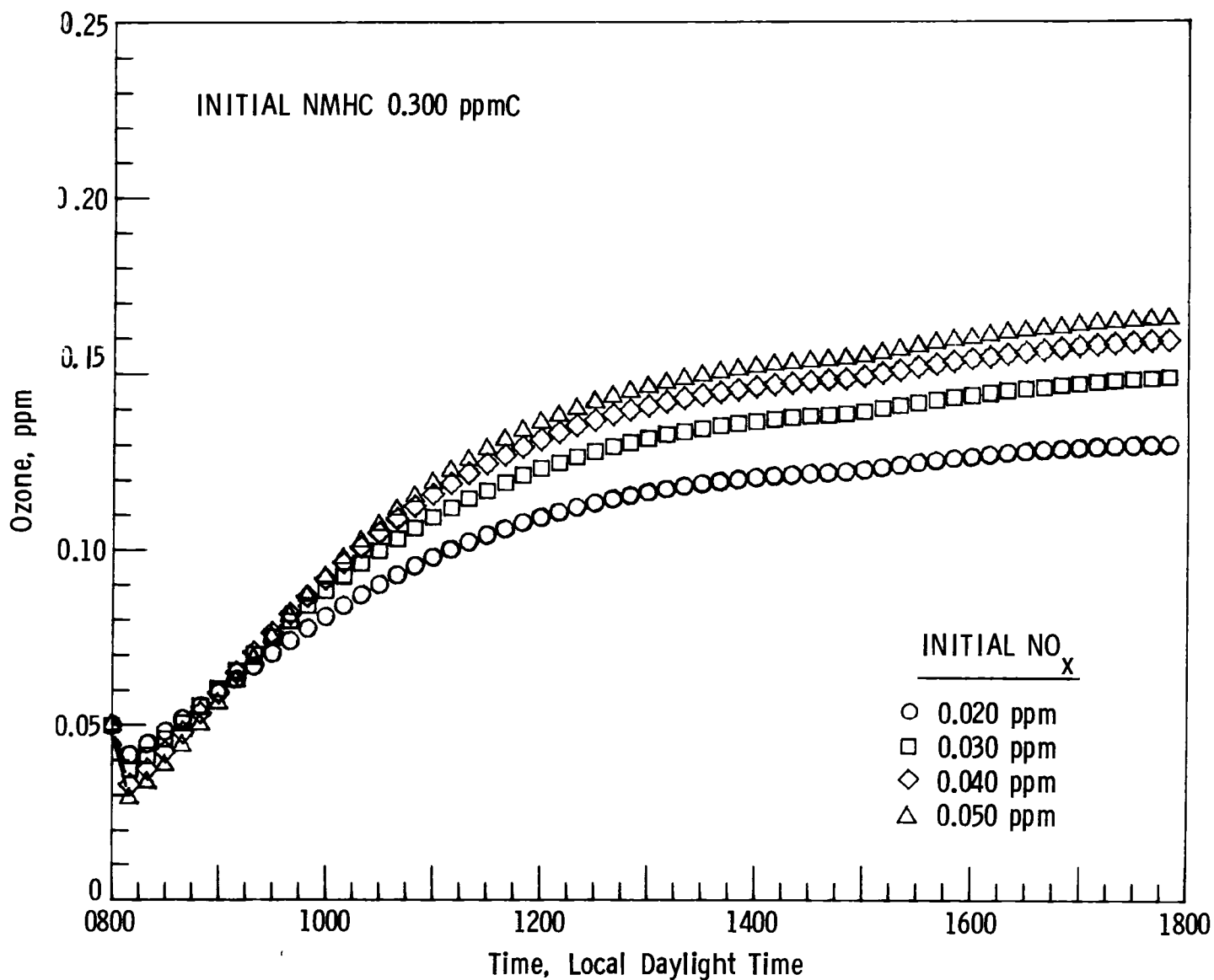


Figure 2c.- Change of O<sub>3</sub> concentration with time for various initial NO<sub>x</sub> concentrations.

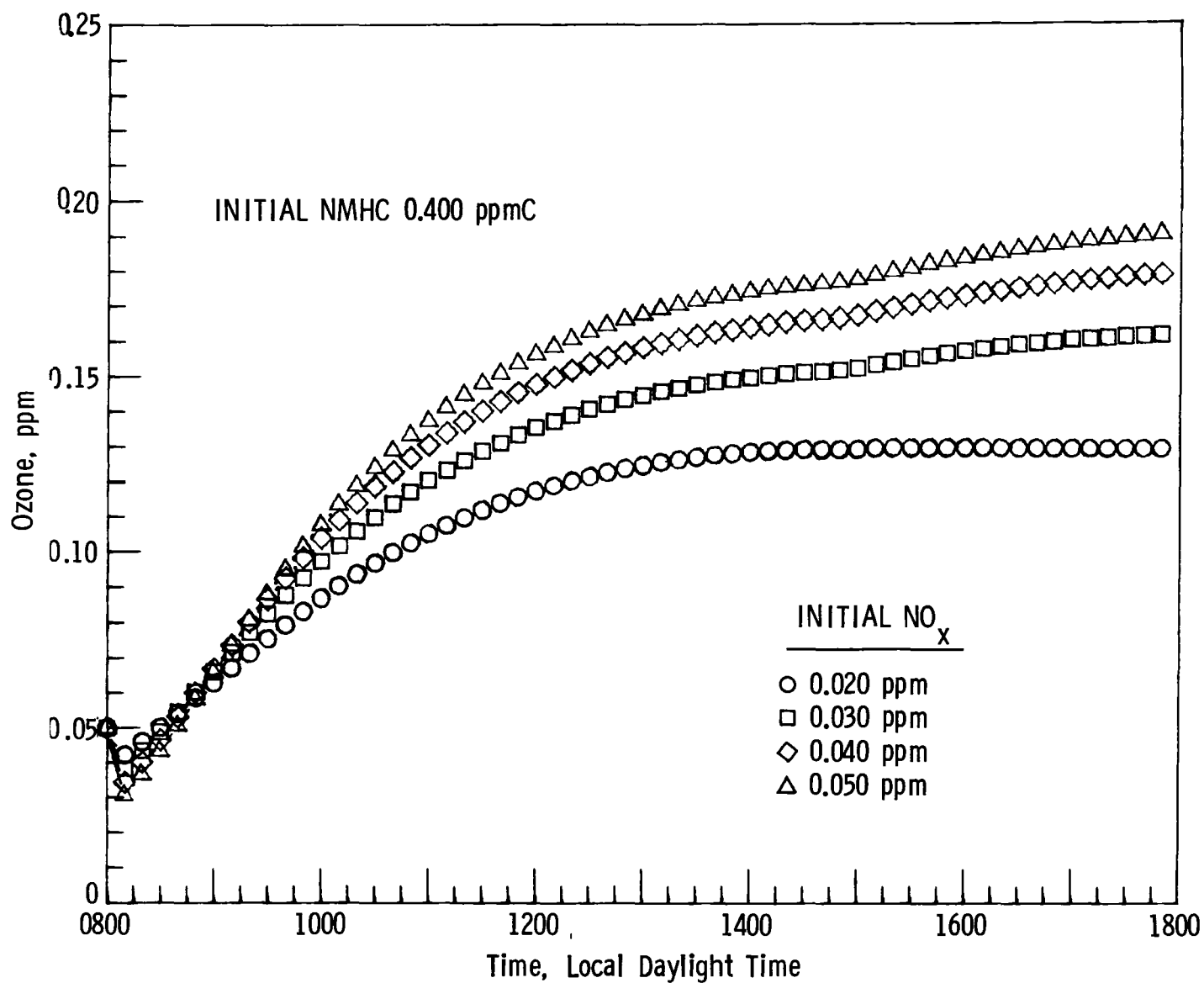


Figure 2d.- Change of O<sub>3</sub> concentration with time for various initial NO<sub>x</sub> concentrations.

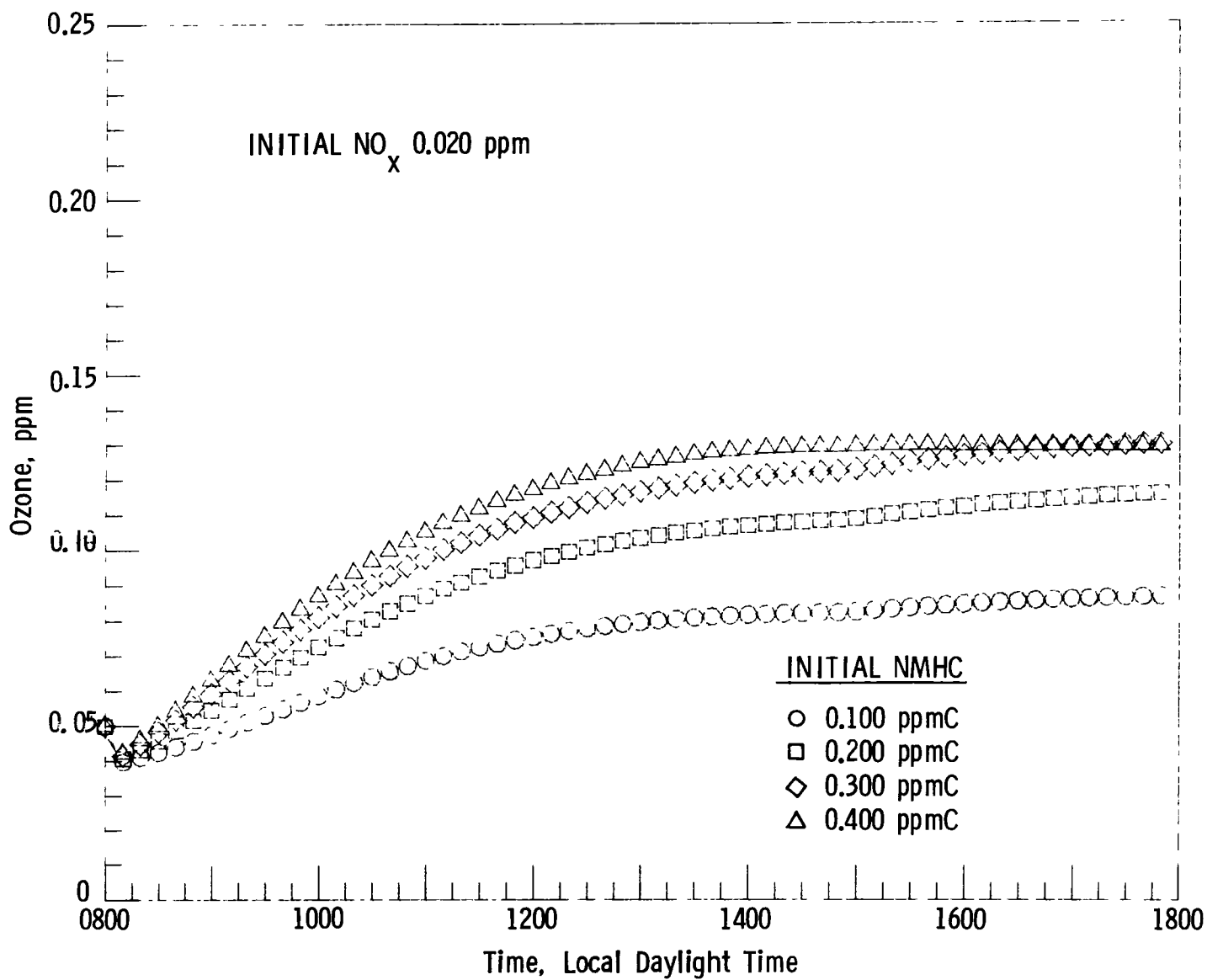


Figure 3a.- Change of O<sub>3</sub> concentration with time for various initial NMHC concentrations.

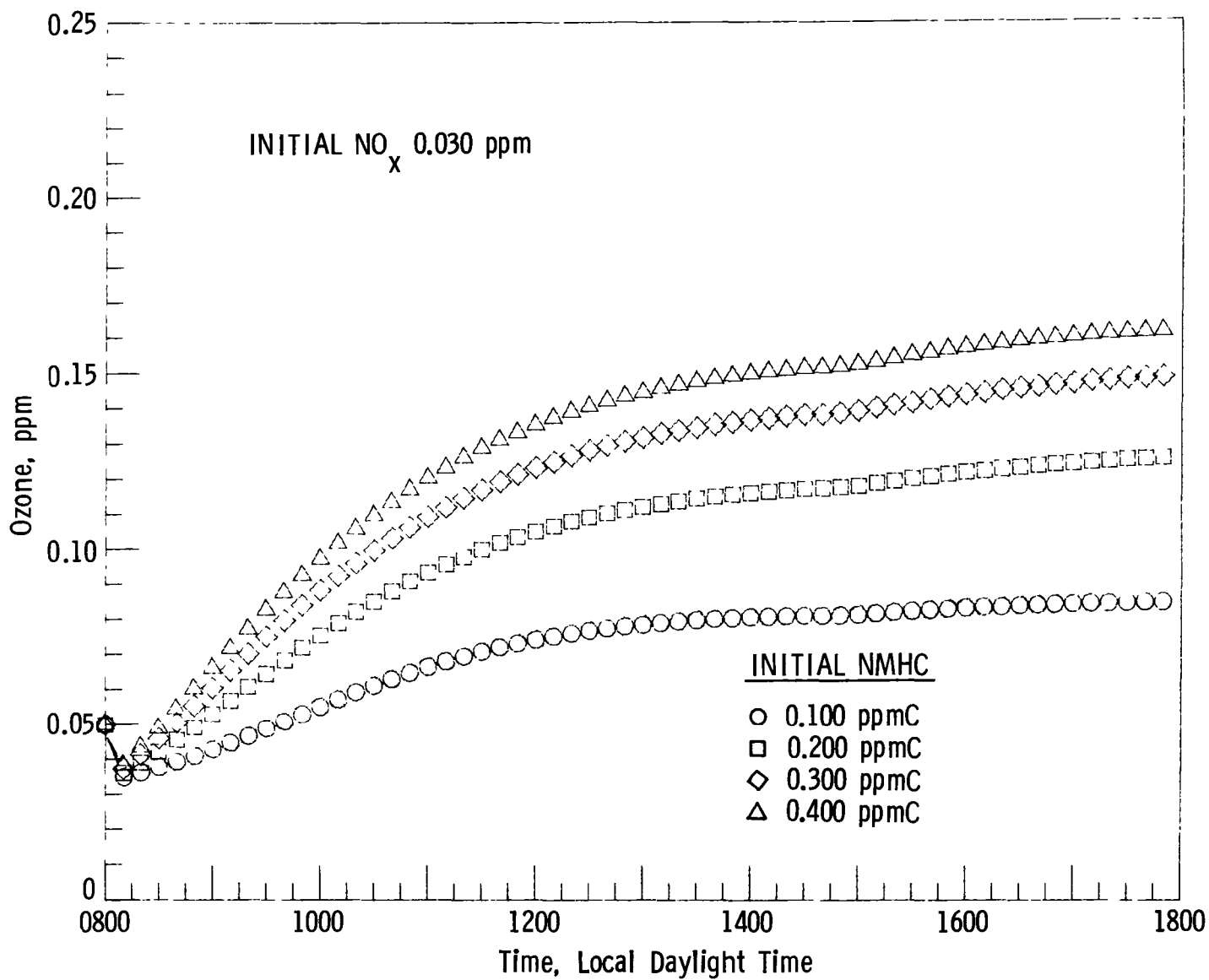


Figure 3b.- Change of O<sub>3</sub> concentration with time for various initial NMHC concentrations.

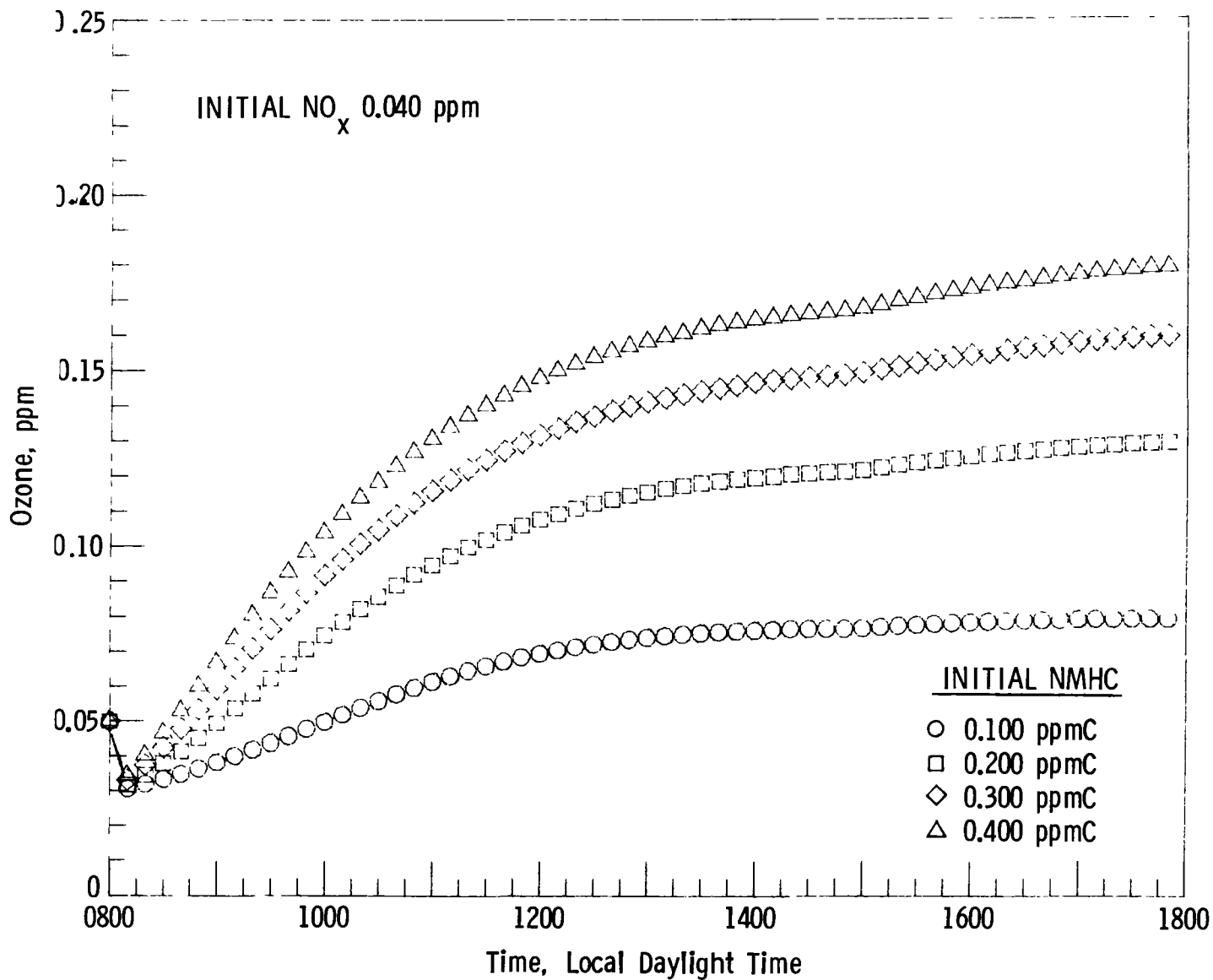


Figure 3c.- Change of  $\text{O}_3$  concentration with time for various initial NMHC concentrations.

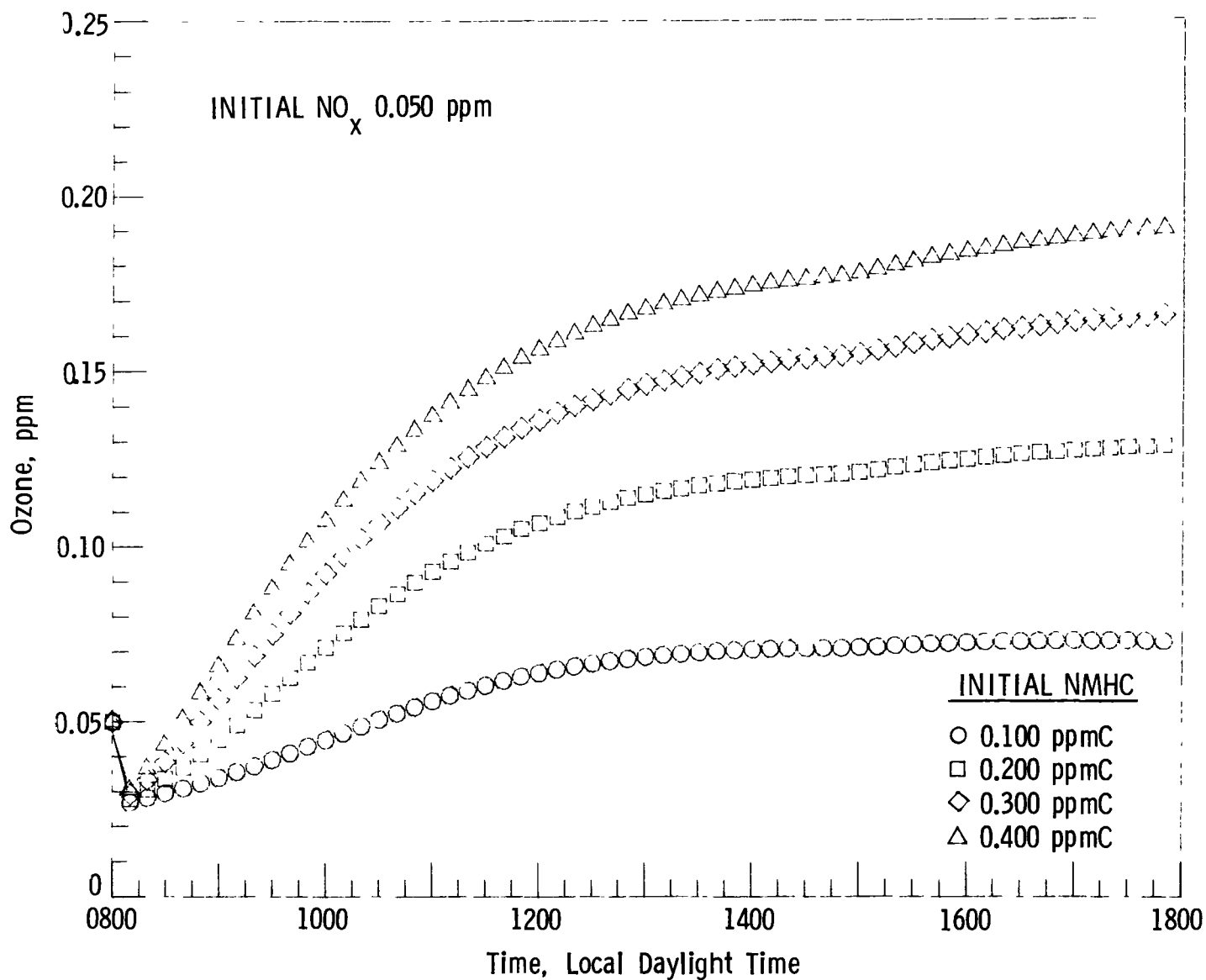


Figure 3d.- Change of  $\text{O}_3$  concentration with time for various initial NMHC concentrations.

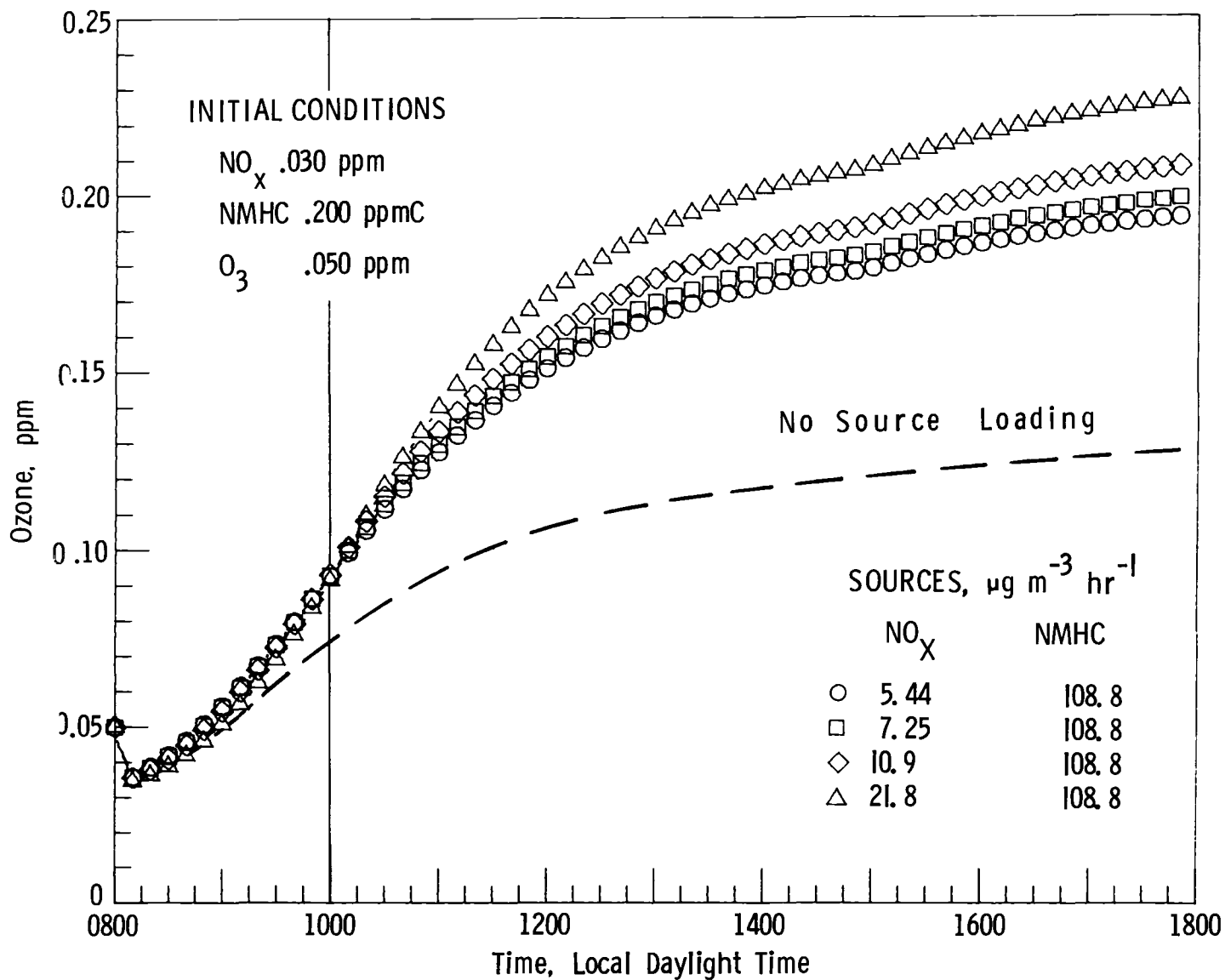


Figure 4.- Change of  $\text{O}_3$  concentration with time for varying source inputs of  $\text{NO}_x$ .



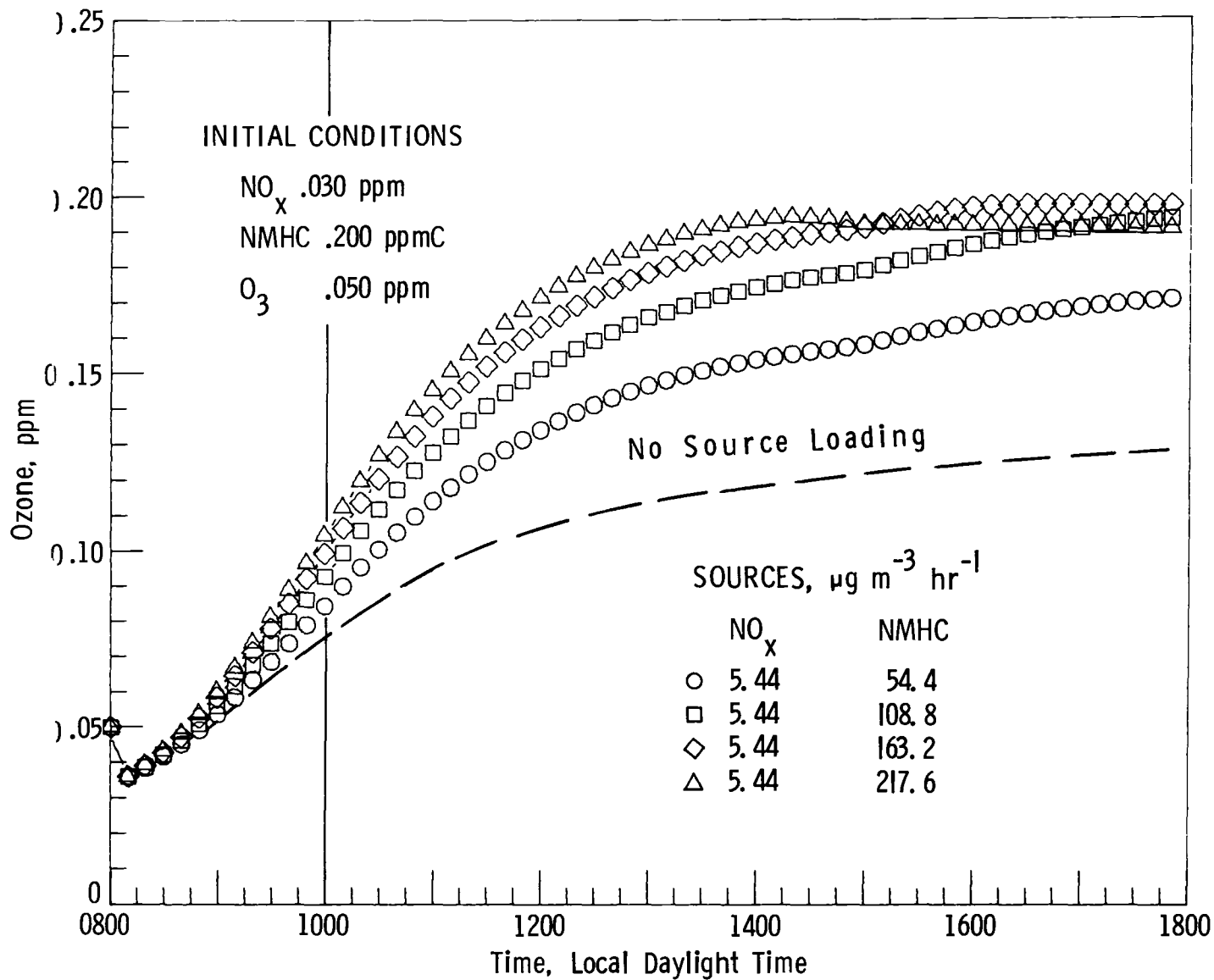


Figure 5.- Change of O<sub>3</sub> concentration with time for varying source inputs of NMHC.

**End of Document**